Available online at www.sciencedirect.com
ScienceDirect
Trans. Nonferrous Met. Soc. China 24(2014) 1307−1316
Transactions of Nonferrous Metals Society of China
www.tnmsc.cn

Effect of post weld heat treatment on properties of variable polarity TIG welded AA2219 aluminium alloy joints

Ji-kun DING[1,2], Dong-po WANG[1,2], Ying WANG[1,2], Hui DU[1,2]

1. School of Materials Science and Engineering, Tianjin University, Tianjin 300072, China;
2. Tianjin Key Laboratory of Advanced Joining Technology, Tianjin 300072, China

Received 4 June 2013; accepted 6 September 2013

Abstract: AA2219 aluminium alloy joints were fabricated by variable polarity tungsten inert gas (VPTIG) welding process and the effects of post weld heat treatment (PWHT) on the tensile properties, microstructure and fatigue behaviour of the welded joints were investigated. The VPTIG welding process was adopted because it could meet the need of cathode cleaning and meanwhile it could reduce the deterioration of tungsten electrode furthest. The welded samples were divided into as-welded (AW) sample and PWHT sample. The PWHT method used on the samples was solution treatment (535 °C, 30 min), water quenching and artificial aging (175 °C, 12 h). The experimental results show that, compared with the AW samples, the microstructure characteristics and mechanical properties of the AA2219 joints after PWHT were significantly improved. The improvement of yield strength, ultimate tensile strength, and fatigue strength are 42.6%, 43.1% and 18.4%, respectively.

Key words: AA2219 aluminium alloy; variable polarity TIG; post weld heat treatment; mechanical properties; microstructure; fatigue behaviour

1 Introduction

Aluminium alloys have been widely used in many fields such as the construction, transportation and aerospace owing to their excellent performance, including light weight, high strength and ductility, good corrosion resistance and abundant resources [1]. Among the various heat-treatable aluminium alloys, AA2219 aluminium alloys possess a good combination of strength and toughness at very low temperature coupled with excellent weldability, which makes this alloy an preferred choice for fabrication of cryogenic storage tanks of launch vehicles [2]. This type of aluminium alloy contains a substantial amount of copper as its major alloying element and minor additions of Mn, Ti, V and Zr [3]. The main strengthening mechanism is precipitation hardening.

Welding is one of the most common joining methods for aluminium alloys. Tungsten inert gas (TIG) process and gas metal arc welding (GMAW) are the most-used welding processes [4]. GMAW possesses advantages of high deposition rate, high welding speed and deep penetration, but excessive heat input brings about grain coarsening and serious distortion, particularly in welding of thin aluminium sheets. Hence, TIG welding process is preferred over gas metal arc welding so as to obtain high quality weldments [5]. The TIG welding used in this work is an improved version known as variable polarity tungsten inert gas (VPTIG). Different from common alternating current TIG welding, VPTIG is able to output controllable current waveform which can reduce deterioration of tungsten electrode furthest under the premises to meet the need of cathode cleaning. Moreover, the output of pulsed current can also strengthen the molten pool stirring to produce refined grains. Although AA2219 aluminium alloy has got an advantage over other series, such as 6000 and 7000 series alloys, in terms of weldability [6,7], it also suffers from a substantial decline in strength after welding. The loss of strength is because the rapid melting and solidification process makes all the strengthening precipitates dissolve into the aluminium matrix and complete dissolution of the precipitates can not take place in weld metal and overaging appear in HAZ and meanwhile solute segregation and grain coarsening also come up [8]. Therefore, the post weld heat treatment (PWHT) can be implemented as an effective method of

Foundation item: Project (51275343) supported by the National Natural Science Foundation of China
Corresponding author: Ying WANG; Tel: +86-22-27405889; Fax: +86-22-27405889; E-mail: wangycl@tju.edu.cn
DOI: 10.1016/S1003-6326(14)63193-9

minimizing the softening and improving the properties of welded joints.

PWHT has been demonstrated to be a practical option to regain the strength of the joints by modifying the size, shape and distribution of the secondary strengthening particles [9]. A few research works have studied the effect of PWHT on the properties of joints welded by different welding processes. The effect of post aging treatment on tensile properties of electron beam welded AA2219 aluminium alloy was reported [10]. The results showed that the yield strength, tensile strength and elongation of the joints after artificially aging (AA) were enhanced. In the AA joints, the precipitates were uniformly distributed along the grain boundaries, forming a continuous network. The influence of three different post weld heat treatments, i.e. solution treatment (ST), artificial aging (AA) and solution treatment followed by artificial aging (STA), on the fatigue behavior of the AA2219 EBW joints was investigated in Ref. [3]. It was found that STA joints exhibited the highest fatigue strength values and lowest fatigue notch factor compared with other joints. A study [11] on AA2219-T6 aluminium alloy joints welded by friction stir welding showed a significant increase in tensile strength and decrease in elongation at fracture after post weld artificial aging treatment at 165 °C for 18 h. The effects of PWHT on the microstructure and the corrosion behaviour of 6061 aluminium alloy joints welded by gas tungsten arc welding (GTAW) were studied [12]. It was found that after PWHT process, the morphology of coarse particles is changed into almost globular shapes from irregular shapes. According to results in Ref. [13], the excellent fatigue property in the post weld aged AA7075 aluminium alloy joints welded by pulsed-current gas tungsten arc welding are attributed to the enhanced mechanical properties, superior microstructures and preferable residual stress field in the weld metal region.

From the literature review, it is understood that most of the published researches have focused on the effect of PWHT on the properties (tensile properties, microstructure characterization and fatigue behaviour) of heat treatable aluminium alloy joints welded by electron beam welding (EBW) or friction stir welding (FSW). However, very few works have been reported on the effect of PWHT on AA2219 aluminium joints welded by VPTIG process. Hence, the present investigation is carried out to study the influence of PWHT on the properties of VPTIG welded AA2219 aluminium alloy joints.

2 Experimental

2.1 Preparation of specimens

AA2219-T87 aluminium alloy with a thickness of 8 mm was used in our experiments. The chemical compositions and mechanical properties of the base metal are listed in Tables 1 and 2, respectively. The rolled AA2219 aluminium alloy plates were cut using an automatic machining tool into two types of required dimensions: 300 mm × 75 mm × 8 mm for butt joint and 300 mm × 150 mm × 8 mm for T-joint welding. The general appearances of these two types of joints are shown in Fig. 1. The welding grooves were done using a milling machine with an angle of 70° for cutting parts of butt joint and 90° for T-joint according to the specification of the single V-groove and K-groove joint, as shown in Fig. 2. Two types of test specimens were prepared: butt joint for tensile test and T-joint for fatigue test. Dimensions of corresponding test specimens are shown in Fig. 3.

The VPTIG welding machine (Miller, USA, Model: Dynasty 700) was used to fabricate the welded joints. The type of filler used for the welding process was

Table 1 Chemical compositions of base metal (mass fraction, %)

Cu	Mn	Fe	Zr	V	Si	Ti	Zn	Al
6.33	0.34	0.13	0.12	0.07	0.06	0.04	0.02	Bal.

Table 2 Mechanical properties of base metal AA2219 alloy

Yield strength/ MPa	Ultimate tensile strength/MPa	Elongation/ %	Vickers hardness $HV_{0.98\,N}$
395	475	10	135

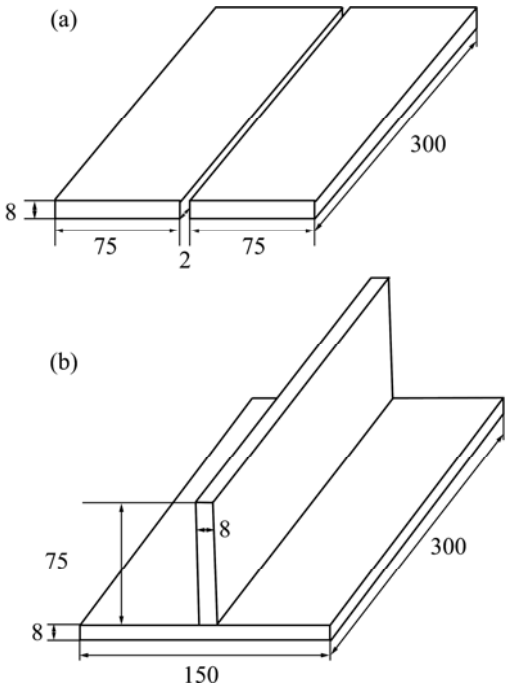

Fig. 1 Geometry of joints (unit: mm): (a) Butt joint; (b) T-joint

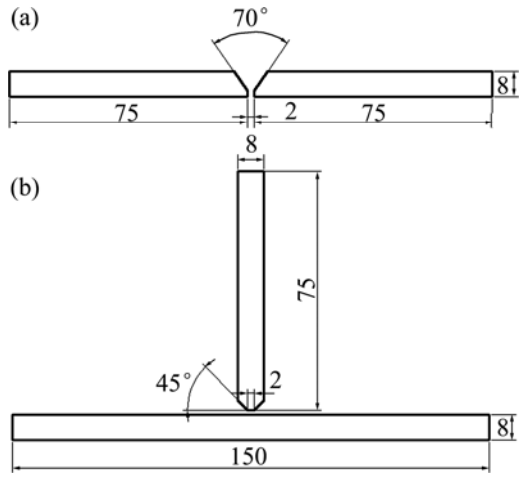

Fig. 2 Two types of grooves (unit: mm): (a) Single V-groove for butt joint; (b) K-groove for T-joint

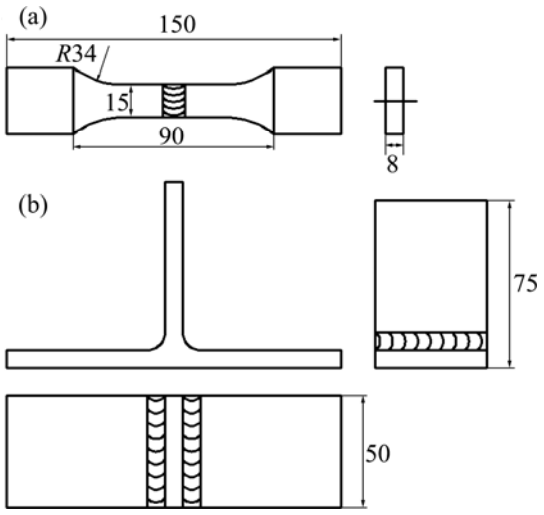

Fig. 3 Dimensions of specimens (unit: mm): (a) Tensile test specimen; (b) Fatigue test specimen

ER2325 with a diameter of 1.6 mm. Before the welding process, the welding parts were wiped with ethanol to remove the impurities on the surface and a motor wire brush was used to remove the oxide. A multi-layer welding project was adopted to ensure full penetration. First tacking welding was used to secure the plates in position and then a three-layer welding was followed immediately. One-side welding was carried out on butt joint and T-joint and both sides of web plate were welded for T-joint. During the process, suitable clamps were taken to avoid welding distortion. The welding condition and process parameters are presented in Tables 3 and 4, respectively.

The welded samples were divided into two groups: as-welded (AW) samples and post weld heat treated (PWHT) samples. For AW joints, the tensile and fatigue tests were performed immediately after welding process. For PWHT joints, heat treatment was conducted before the latter tests. The PWHT methods were solution treatment, water quenching and artificial aging.

Solution treatment was performed at 535 °C for a soaking time of 30 min. The atmosphere box furnace (Model: HMX1100−30A) was used to heat the joints from room temperature to 535 °C at a rate of 10 °C/min. Then, the samples were taken out of the furnace and put into a water bath for quenching. Artificial aging was carried out at 175 °C for a soaking time of 12 h. The quenched joints were heated in the furnace from room temperature to 175 °C at a rate of 10 °C/min. After the soaking time, the joints were slowly cooled in the furnace to room temperature and the whole PWHT process was completed.

2.2 Property tests

The tensile test specimens were taken from the welded joints in the transverse direction (normal to the

Table 3 Welding condition and process parameters for butt joint

Welding layer	Current/A	Voltage/V	Current frequency/Hz	Pulse frequency/Hz	Peak pulse duration/%	Base pulse value to peak pulse value/%	Gas flow rate/($L \cdot min^{-1}$)
Tacking	140	13.0	100	6	70	20	15
First	150	10.6	100	6	70	20	15
Second	155	12.9	100	−	−	−	15
Third	157	12.4	100	−	−	−	15

Table 4 Welding condition and process parameters for T- joint

Welding layer	Current/A	Voltage/V	Current frequency/Hz	Pulse frequency/Hz	Peak pulse duration/%	Base pulse value to peak pulse value/%	Gas flow rate/($L \cdot min^{-1}$)
Tacking	160	14.2	100	6	70	20	15
First	225	13.5	100	6	70	20	15
Second	225	13.1	100	−	−	−	15
Third	196	12.8	100	−	−	−	15

welding direction) and a super CNC wire cutting machine was used to machine the samples into the required dimensions. Tensile test was performed on an electro-mechanically controlled universal testing machine (Model: YDL−2000, China). The loading speed was 1 mm/s. The 0.2% offset yield strength, ultimate tensile strength and elongation were evaluated for tensile specimens. The fractured surface of the tensile tested specimens was analyzed using a Hitachi-S4800 scanning electron microscope (SEM) to investigate the fracture morphology.

The welded joints, comprising of weld metal, HAZ, base metal regions, were cut into required sizes and then polished with different grades of emery papers and polishing machine. After finishing polishing, specimens were etched with Keller's reagent to reveal the microstructure. The microstructural analysis was conducted using an Olympus-GX51 optical microscope and the precipitates of the matrix were observed using SEM. A digital Vickers microhardness tester (Model: MHV 2000) was used to measure the hardness across the joints with a load of 0.98 N. The specific locations were separated into three parts: Base metal (BM), HAZ and weld metal (WM), as shown in Fig. 4. In addition, the impact test was also conducted on the JB-300B impact testing machine at 25 °C.

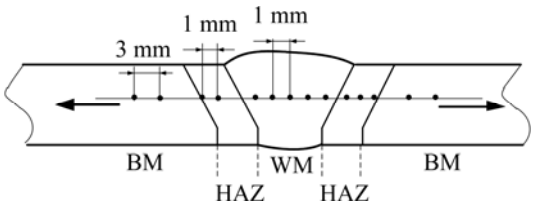

Fig. 4 Locations of hardness measurement across welded joints

Fatigue test specimens were prepared from welded joints in the transverse direction to evaluate the fatigue behaviour (S−N curve). The tests were performed on a 100 kN high frequency fatigue testing machine (Model: PLG-200C, China) at different stress levels and all the fatigue tests were carried out under four-point bending loading condition (Fig. 5) with a stress ratio of 0.5. The static load accuracy for the full range of the testing machine was 0.2% and the accuracy of the dynamic load amplitude of vibration was 2%. For each type of sample, ten specimens were tested and the test data were used to plot S−N curves.

3 Results

3.1 Tensile properties and hardness

The tensile properties, such as yield strength, tensile strength and elongation of the joints in AW and PWHT conditions were evaluated. All the data were the average of three measured values presented in Table 5.

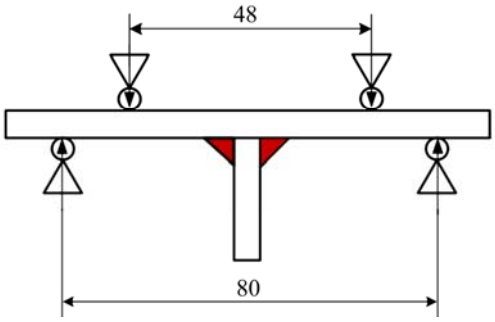

Fig. 5 Sketch of four-point bending loading (unit: mm)

Table 5 Tensile properties of base metal (BM), as-welded (AW) and post weld heat treated (PWHT) samples

Sample	Yield strength/ MPa	Ultimate tensile strength/ MPa	Elongation/ %	Joint efficiency/ %
BM	395	475	15	−
AW	202	253	9.1	53.3
PWHT	288	362	11.5	76.2

The yield and ultimate tensile strength of PWHT sample were 288 MPa and 362 MPa respectively and those in AW sample were 202 MPa and 253 MPa, respectively. It was observed that the post weld heat treatment exhibited an increment of 42.6% and 43.1% in yield and ultimate tensile strength compared with as-welded condition, respectively. The elongations for PWHT and AW samples were 11.5% and 9.1%, respectively and thus, a 26.4% increment was achieved when implementing PWHT on the welded joints. This could be explained by the fact that the ductility of the material is obtained from the solution heat treatment for aluminium alloys [14]. At the solution temperature (535 °C), $CuAl_2$ precipitates completely dissolved into the aluminium matrix of AA2219 alloy and the material was held at this temperature for enough time, producing a uniform phase [15]. The increase in ductility was mainly attributed to a reduction of crystalline lattice defects, which makes it easier for crystal slip (i. e. dislocation motion).

The joint efficiency is defined as the ratio of an ultimate tensile strength of welded joint to that of base metal. The joint efficiency of AW sample is merely 53.3% while the PWHT sample offers joint efficiency of 76.2%, which is significantly increased by 43.1% compared with the AW sample. From the experimental data, it is very clear that the tensile properties of AA2219 welded joints have been apparently reduced by VPTIG welding while the post weld heat treatments used in this study have improved the tensile properties to a great extent.

A Vickers microhardness test was done at the middle of the transverse plane across the welded joints.

The microhardness profiles for base metal, as-welded and post weld heat treated joints are shown in Fig. 6. The average hardness of base metal in its initial T87 condition was approximately HV 135. For as-welded samples, the minimum hardness value was located in weld metal (WM) zone, which may be owing to the formation of very fine recrystallized grains. The average microhardness values in WM and HAZ of as-welded joints (HV 75.6 and HV 82.2) were 44.6% and 39.7% lower than that in base metal (HV 136.4). The minimum value (HV 69.8) present in the WM region was only 51.2% that of base metal. The microhardness of the as-welded joints after post weld heat treatment was drastically increased. As a result, a flat microhardness profile was obtained, except in WM where the lowest microhardness value of HV 129.3 can be seen. The average hardness value of PWHT joints was improved to HV 133.7, roughly equal to 98% of base metal hardness. The post weld heat treatment significantly hardened the welded joints in all zones as can be drawn from their higher microhardness than that of the as-welded joints.

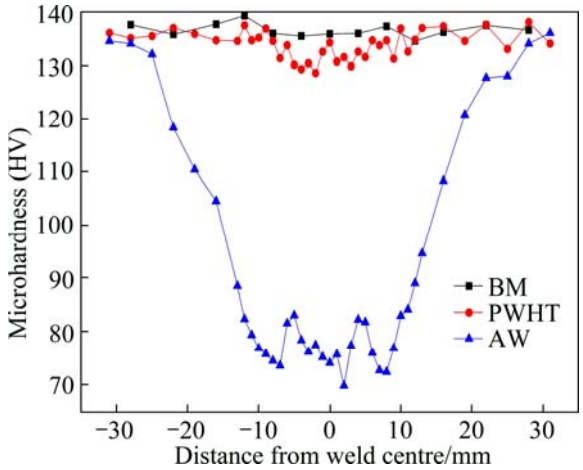

Fig. 6 Variation of microhardness for as-welded (AW), post weld heat treated (PWHT) samples and base metal (BM)

The impact toughness values are listed in Table 6. From Table 6, it can be seen that the impact toughness of BM sample was the highest (12.9 J/cm^2). The impact toughness of AW sample was 9.2 J/cm^2, reduced by 29% compared with BM. However, the impact toughness of PWHT sample was 14.2 J/cm^2, increased by 10% compared with BM.

3.2 Fracture surface

The fractographs of base metal, AW sample and PWHT samples are presented in Fig. 7. All the welded joints failed in the weld metal region and for specimens of base metal, necking was observed during tensile test and the fracture surface was inclined at 45° to the loading axis. As can be seen from Fig. 7, the fractographs

Table 6 Impact toughness of different samples

Sample No.		Impact toughness/ (J·cm^{-2})	Average value/ (J·cm^{-2})
BM	1	12.5	12.9
	2	12.5	
	3	13.8	
AW	1	10.0	9.2
	2	8.7	
	3	8.8	
PWHT	1	15.0	14.2
	2	15.0	
	3	12.5	

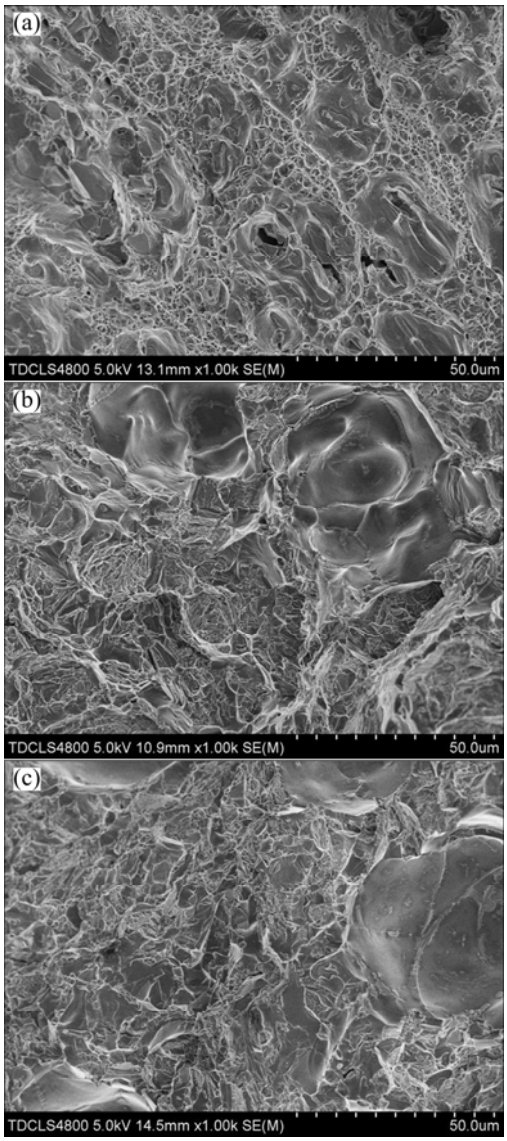

Fig. 7 Fractographs of tensile specimens: (a) Base metal; (b) AW sample; (c) PWHT sample

of three types of samples invariably contain dimples, indicating that the fracture pattern is mostly ductile. In Fig. 7(a), the dimples on the fracture surface of base

metal are fine and uniformly distributed over the surface. Since fine dimples are an indication of high ductile material, base metal shows a relatively high ductility compared to the other two types of welded joints. This is also in agreement with the highest elongation of the base metal. For tensile test of ductile material, voids generally form prior to necking while if a neck is formed earlier, the void formation becomes much more prominent [16]. The dimples are coarse and elongated in the AW sample (Fig. 7(b)) whereas fine dimples are seen in the PWHT sample (Fig. 7(c)). As mentioned above, fine dimples are the evidence of highly ductile materials and meanwhile considering the higher impact toughness of PWHT sample, the ductility of welded joints has been enhanced by post weld heat treatment.

3.3 Microstructure

The optical micrographs of the microstructure of welded joints are displayed in Fig. 8. The PWHT samples contain fine, equiaxed and uniformly distributed grains in the weld metal (WM) region (Fig. 8(c)) compared to AW sample (Fig. 8(a)). Combining Figs. 8(a) and (c), it also can be seen that the grains of weld metal of AW sample appear to be slightly elongated but the change in the grain size of two types of samples is not obvious, indicating that the post weld heat treatment did not lead to substantial grain growth in this investigation. The main strengthening precipitate in AA2219 aluminium alloy is $CuAl_2$ whose formation and distribution throughout alloy matrix depend on the solution treatment and aging treatment [4]. The AW sample (Fig. 8(a)) exhibits widely spaced and less dense precipitates while the PWHT sample (Fig. 8(c)) exhibits uniformly distributed and dense precipitates within the grains and along grain boundaries. This suggests that there is a significant increase in the number of precipitates after the post weld heat treatment.

The SEM images of HAZ in AW and PWHT samples are presented in Fig. 9. It is confirmed that the particles marked with circles are Al−Cu precipitates. In the AW sample, the precipitates are large, few and far (Fig. 9(a)), while in PWHT sample, the precipitates are fine, small and more than that in the as-welded sample (Fig. 9(b)).

Microstructure and property of HAZ were definitely changed due to the effect of welding thermal cycle. Compared with the grain size in WM, the grains of HAZ become larger as shown in Figs. 8(b) and (d). Meanwhile, the precipitates also gather and grow to large size and all these changes lead to properties deterioration.

3.4 Fatigue behaviour

Tables 7 and 8 show the fatigue test results of as-welded (AW) and post weld heat treated (PWHT) samples, including fatigue life and fracture location under different stress levels. These data are used to plot S−N curves to reveal the effect of post weld heat treatment on the welded joints.

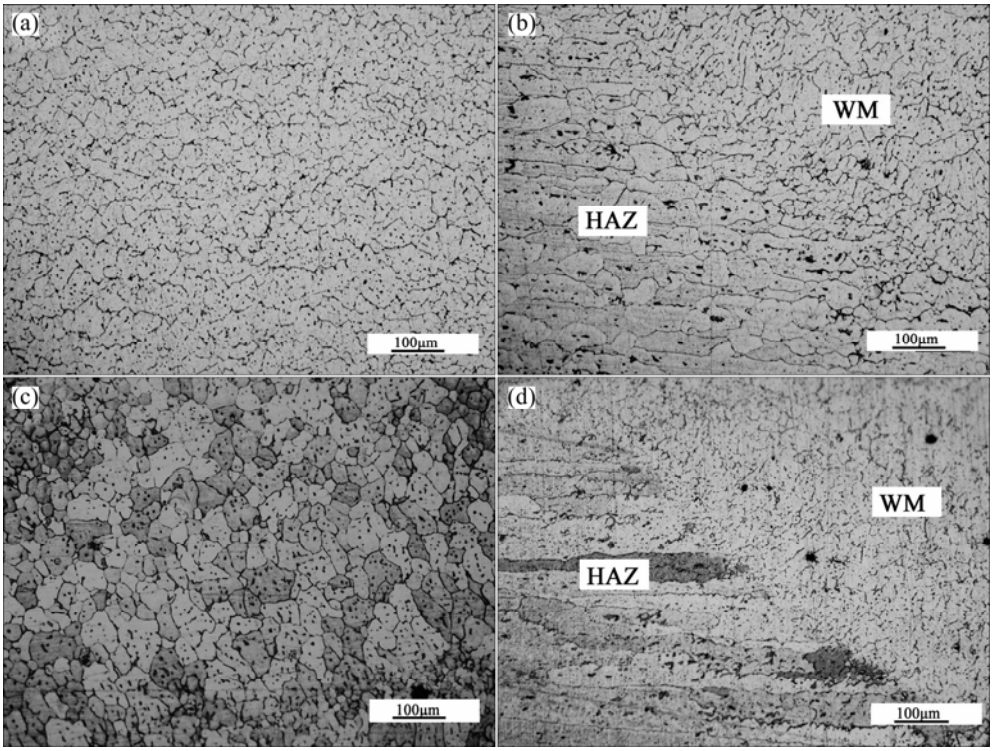

Fig. 8 Optical micrographs in different regions of AW and PWHT samples: (a) WM of AW; (b) HAZ of AW; (c) WM of PWHT; (d) HAZ of PWHT

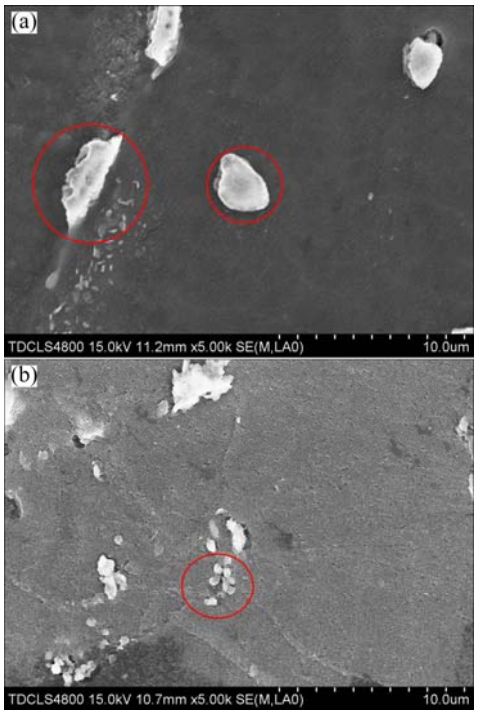

Fig. 9 SEM images of HAZ in different samples: (a) AW sample; (b) PWHT sample

Table 7 Fatigue test results of AW samples

No.	Stress range, $\Delta\sigma$/MPa	Fatigue life/10^6	Fracture location
1	190	0.064	Weld toe
2	165	0.203	Weld toe
3	165	0.220	Weld toe
4	140	0.692	Weld toe
5	145	0.354	Weld toe
6	105	0.953	Weld toe
7	115	0.430	Weld toe
8	100	3.217	Weld toe
9	85	2.856	Weld toe
10	85	4.362	Weld toe

Table 8 Fatigue test results of PWHT samples

No.	Stress range, $\Delta\sigma$/MPa	Fatigue life/10^6	Fracture location
1	190	0.096	Weld toe
2	170	0.304	Weld toe
3	170	0.521	Weld toe
4	140	0.987	Weld toe
5	140	0.578	Weld toe
6	115	1.073	Weld toe
7	110	2.125	Weld toe
8	95	5.845	Weld toe
9	85	3.775	Weld toe
10	80	7.812	Weld toe

Fatigue testing data are analyzed according to the guideline of statistical method [17] recommended by the International Institute of Welding (IIW).

Figure 10 shows the corresponding S−N curves both for AW samples and PWHT samples. The stress range corresponding to 2×10^6 cycles is considered an indication of the fatigue strength and it has been evaluated for all the samples and is presented in Table 9. As can be seen in Fig. 10, the mean S−N curve of PWHT samples is much higher and thus under the same stress level, fatigue life of AW samples is much shorter than that of the PWHT samples. The fatigue strength of AW sample is 98 MPa while the fatigue strength of PWHT sample is 116 MPa. Therefore, 18.4% increment of fatigue strength is achieved when the post weld heat treatment is implemented on the welded joints.

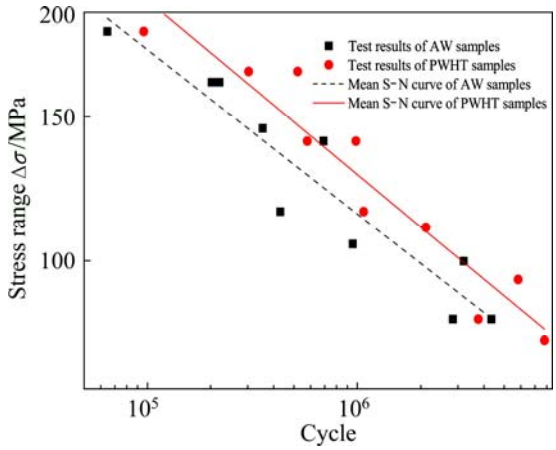

Fig. 10 S−N curves of AW and PWHT samples

Table 9 Statistical result of fatigue test data

Sample	Slope of S−N curve, m	Intercept of S−N curve, C_m	Standard deviation, S_c	Fatigue strength $\Delta\sigma_m$ at 2×10^6 cycles/MPa
AW	5.02	2.13×10^{16}	1.60	98
PWHT	4.74	9.57×10^{15}	1.53	116

4 Discussion

4.1 Effect of post weld heat treatment on tensile properties

Based on the experimental results, it is very obvious that tensile properties (yield strength, ultimate tensile strength and elongation) of AA2219 aluminium alloy joints have been reduced after VPTIG welding. However, the post weld heat treatment shows a significant improvement on the tensile properties of VPTIG welded AA2219 aluminium alloy joints (seen Table 5). Like the tensile properties, the microhardness across transverse cross section of welded joints also shows a trend of sharp increases after PWHT (Fig. (6)). In general, strength is

positively related to hardness and this is in accordance with the experimental data. The fracture location of all the tensile specimens is weld metal zone, indicating that weld metal zone is the weakest part of the joints. This could be explained by the microhardness measurement results that weld metal shows a lower hardness than any other regions. PWHT samples contain finer dimples than as-welded samples, which explain the increase in elongation and impact toughness of welded joints after post weld heat treatment (Fig. (7)).

According to the results of HUANG and KOU [18,19], the size and distribution of $CuAl_2$ play a major role in deciding the tensile properties and hardness of the welds of AA2219 aluminium alloy. Fine, equiaxed and uniformly distributed grains can be observed in the micrograph (Fig. 8(c)) and heat treatment does not result in substantial grain growth due to the proper soaking time (30 min) in solution treatment step. In AA2219 alloy, the strengthening precipitate is $CuAl_2$ and fine uniformly distributed $CuAl_2$ precipitates explain the superior tensile properties and higher microhardness in base metal and heat treated joints than in as-welded joints. This is also evident from earlier research by MALARVIZHI et al [3] who attributed the superior tensile and hardness properties of solution and artificial aged joints to fine and uniform distribution of precipitates in the weld metal region. Similar conclusions were also drawn from other investigation results [20,21] that fine dimples increase the tensile strength and hardness and this was attributed to precipitation hardening in the weld metal region after PWHT.

The precipitates form from solution treatment and subsequent artificial aging. At 535 °C, the $CuAl_2$ precipitates completely dissolve into the aluminium matrix of AA2219 alloy [15]. The strength of the PWHT AA2219 welded joints is improved with the following artificial aging which is an atom diffusion process. Supersaturated vacancies and solute atoms are produced in the solid solution phase during the process of solution treatment. The presence of high concentration vacancies and solute supersaturation promotes the rapid nucleation of GP zones in the early stages of artificial aging [9]. The GP zones, with no independent crystal structure, are coherent with the aluminium matrix, resulting from copper atoms segregation formed along {100} lattice planes [22]. With the increase of artificial aging time, some of the primary GP zones are replaced by transient phase θ'' precipitates, which causes a substantial increase in the density of distortion of lattice planes and hindering of dislocation movement. This explains why the tensile properties and hardness of welded joints are dramatically enhanced by the post weld heat treatment. The strengthening effect can also be the result of interference with the motion of the dislocation because of the formation of precipitates. Moreover, in artificially aged joints, the precipitates are very fine and uniformly distributed throughout the matrix. This also leads to an increase in dislocation density, which results in an improvement in enhanced tensile properties and hardness [23]. MALARVIZHI et al [3] also found the similar trend of results for electron beam welded joints and reported that ultimate tensile strength, yield strength and elongation all increased after artificial aging. During the welding, these precipitates are assumed to dissolve and the weld metal should be left devoid of any precipitates [24]. However, after welding was completed, a small number of precipitates were present in the weld metal of as-welded samples (Fig. 8(a)) and these precipitates were widely spaced and less than in PWHT samples (Fig. 8(c)). Therefore, it is possible that the precipitate particles in weld metal could result from natural aging after they have mostly melted during welding process. Because of the rapid melting and solidification during the welding process, complete dissolution of the precipitates could not happen [25] and this is the main reason for lower tensile properties and hardness of VPTIG welded joints in as welded condition.

If the soaking time of artificial aging continues to increase, θ'' precipitates will transform into another formation known as θ' precipitates which are semi-coherent with the aluminium matrix. θ' phase has tetragonal lattice structure, producing less lattice distortion and thus strengthening effect weakens. The overaging phenomenon occurs in this stage and materials become soft. Due to the welding heat, the overaging happens in the HAZ and this explains the coarsening of grains and precipitates in AW joints. Correspondingly, tensile and hardness properties also decrease as a result of overaging in the HAZ. Further soaking will lead to generation of the final stable θ phase which is completely incoherent with the aluminium matrix. The appearance of θ phases indicates a significant drop in strength and hardness of materials. Hence, the artificial aging will generally not reach to this stage.

4.2 Effect of post weld heat treatment on fatigue behaviour

From the fatigue test results and S−N curves, it is obvious that the post weld heat treatment can significantly improve the fatigue life of the VPTIG welded joints of AA2219 aluminium alloy. The reason for better fatigue performance of PWHT samples can be summarized as good tensile properties in the heat treated joints, fine microstructure in the weld metal region and the large amount of fine and uniformly distributed strengthening precipitates in the aluminium matrix. This is also evident from Ref. [6] in which the influence of post weld heat treatment on fatigue crack growth

behaviour of electron beam welded AA2219 alloy was discussed. Higher tensile and yield strength are very useful to increase fatigue limit of the PWHT sample and therefore the fatigue crack initiation is delayed. Higher elongation implies higher ductility and also leads to more resistance to fatigue crack propagation and fatigue crack growth rate is consequently lower for the PWHT samples. Thus, the double effect of the higher tensile strength and higher ductility of the PWHT joint provide intense barrier to crack initiation and propagation, and finally the post weld heat treatment improves the fatigue properties of the welded joints. Fine grains, with large grain boundary area in PWHT weld metal, on one hand, produce a strengthening effect, and on the other hard, offer more resistance to the fatigue cracks growth. Furthermore, the grain boundaries are abundant in stored energy which can offer more resistance to the growing fatigue cracks than grain interior [26]. This could explain why fatigue behaviour of PWHT joints is superior to that of as-welded joints.

The size and distribution of strengthening precipitates also have an effect on the fatigue crack growth behaviour of welded joints [27]. In the weld metal region of PWHT samples, fine and uniform distribution of precipitates is throughout the aluminium matrix, which explains the enhanced tensile properties and hardness compared to AW joints. Similar to fine grains, the uniformly distributed fine precipitate particles could also hinder fatigue crack growth and thus delay the crack propagation rate [18]. Based on this, the enhanced fatigue performance is obtained in PWHT joints.

5 Conclusions

1) The post weld heat treatment significantly improved yield and ultimate tensile strength by 42.6% and 43.1% respectively; a 26.4% increment in elongation was achieved and the average hardness value was increased to 98% of base metal hardness. These results indicate that PWHT was able to enhance the tensile and hardness properties of VPTIG welded AA2219 aluminium alloy joints.

2) Finer dimples were seen in the fractograph of PWHT tensile specimen in accordance with achieved indicating higher ductility. Higher elongation and impact toughness were also obtained by implementing post weld heat treatment. Uniformly distributed fine grains were observed for the PWHT samples, and in the aluminium matrix, a number of precipitates were distributed within the grains and along grain boundaries. These resulted in the superior tensile and hardness properties, compared to the AW joints.

3) An 18.4% increase in fatigue strength was achieved when implementing PWHT on the welded joints and the better fatigue performance was attributed to the enhanced tensile properties and preferable microstructure in the weld metal region of the PWHT samples.

References

[1] AHMAD R, BAKAR M A. Effect of a post-weld heat treatment on the mechanical and microstructure properties of AA6061 joints welded by the gas metal arc welding cold metal transfer method [J]. Materials & Design, 2011, 32(10): 5120−5126.

[2] HARTMAN J A, BEIL R J, HAHN G T. Effect of copper-rich regions on tensile properties of VPPA weidments of 2219-T87 aluminum [J]. Welding Journal, 1987, 66(3): s73−s83.

[3] MALARVIZHI S, RAGHUKANDAN K, VISWANATHAN N. Fatigue behaviour of post weld heat treated electron beam welded AA2219 aluminium alloy joints [J]. Materials & Design, 2008, 29(8): 1562−1567.

[4] KIM H T, NAM S W. Solidification cracking susceptibility of high strength aluminum alloy weldment [J]. Scripta Materialia, 1996, 34(7): 1139−1145.

[5] MANTI R, DWIVEDI D K, AGARWAL A. Pulse TIG welding of two Al−Mg−Si alloys [J]. Journal of Materials Engineering and Performance, 2008, 17(5): 667−673.

[6] MALARVIZHI S, RAGHUKANDAN K, VISWANATHAN N. Investigations on the influence of post weld heat treatment on fatigue crack growth behaviour of electron beam welded AA2219 alloy [J]. International Journal of Fatigue, 2008, 30(9): 1543−1555.

[7] MALARVIZHI S, BALASUBRAMANIAN V. Fatigue crack growth resistance of gas tungsten arc, electron beam and friction stir welded joints of AA2219 aluminium alloy [J]. Materials & Design, 2011, 32(3): 1205−1214.

[8] TOSTO S, NENCI F, HU J. Microstructure and properties of electron beam welded and post-welded 2219 aluminium alloy [J]. Materials Science and Technology, 1996, 12(4): 323−328.

[9] SHARMA C, DWIVEDI D K, KUMAR P. Effect of post weld heat treatments on microstructure and mechanical properties of friction stir welded joints of Al−Zn−Mg alloy AA7039 [J]. Materials & Design, 2013, 43(1): 134−143.

[10] MALARVIZHI S, RAGHUKANDAN K, VISWANATHAN N. Effect of post weld aging treatment on tensile properties of electron beam welded AA2219 aluminum alloy [J]. International Journal of Advanced Manufacturing Technology, 2008, 37(3−4): 294−301.

[11] LIU H J, CHEN Y C, FENG J C. Effect of heat treatment on tensile properties of friction stir welded joints of 2219-T6 aluminium alloy [J]. Materials Science and Technology, 2006, 22(2): 237−241.

[12] NIKSERESHT Z, KARIMZADEH F, GOLOZAR M A, HEIDARBEIGY M. Effect of heat treatment on microstructure and corrosion behavior of Al6061 alloy weldment [J]. Materials and Design, 2010, 31(5): 2643−2648.

[13] BALASUBRAMANIAN V, RAVISANKAR V, REDDY G M. Influences of pulsed current welding and post weld aging treatment on fatigue crack growth behaviour of AA7075 aluminium alloy joints [J]. International Journal of Fatigue, 2008, 30(3): 405−416.

[14] GARRETT R P, LIN J, DEAN T A. An investigation of the effects of solution heat treatment on mechanical properties for AA 6xxx alloys: Experimentation and modelling [J]. International Journal of Plasticity, 2005, 21(8): 1640−1657.

[15] HUANG C, KOU S. Partially melted zone in aluminum welds—Liquation mechanism and directional solidification [J]. Welding Journal, 2000, 79(5): s113−s120.

[16] BALASUBRAMANIAN V, RAVISANKAR V, REDDY G M. Effect of pulsed current and post weld aging treatment on tensile properties

of argon arc welded high strength aluminium alloy [J]. Materials Science and Engineering A, 2007, 459(1−2): 19−34.
[17] HOBBACHER A. Recommendations on fatigue design of welded joints and components [C]//XIII-2151r4-07/XV-1254r4-07. Paris: International Institute of Welding, 2008.
[18] HUANG C, KOU S. Liquation cracking in full-penetration Al−Cu welds [J]. Welding Journal, 2004, 83(2): s50−s58.
[19] HUANG C, KOU S. Partially melted zone in aluminum welds-planar and cellular solidification [J]. Welding Journal, 2001, 80(1): s46−s53.
[20] AKHTER R, IVANCHEV L, BURGER H P. Effect of pre/post T6 heat treatment on the mechanical properties of laser welded SSM cast A356 aluminium alloy [J]. Materials Science and Engineering A, 2007, 447(1−2): 192−196.
[21] HU B, RICHARDSON I M. Microstructure and mechanical properties of AA7075(T6) hybrid laser/GMA welds [J]. Materials Science and Engineering A, 2007, 459(1−2): 94−100.
[22] HUANG C, KOU S. Partially melted zone in aluminum welds: Solute segregation and mechanical behavior [J]. Welding Journal, 2001, 80(S): 9−17.
[23] ELANGOVAN K, BALASUBRAMANIAN V. Influences of post-weld heat treatment on tensile properties of friction stir-welded AA6061 aluminum alloy joints [J]. Materials Characterization, 2008, 59(9): 1168−1177.
[24] LIN D C, WANG G X, SRIVATSAN T S. A mechanism for the formation of equiaxed grains in welds of aluminum–lithium alloy 2090 [J]. Materials Science and Engineering A, 2003, 351(1−2): 304−309.
[25] DAVID S A, VITEK J M. Correlation between solidification parameters and weld microstructures [J]. International Materials Reviews, 1989, 34(5): 213−245.
[26] MALARVIZHI S, BALASUBRAMANIAN V. Effect of welding processes on AA2219 aluminium alloy joint properties [J]. Transactions of Nonferrous Metals Society of China, 2011, 21(5): 962−973.
[27] STANZL-TSCHEGG S E, PLASSER O, TSCHEGG E K, VASUDEVAN A K. Influence of microstructure and load ratio on fatigue threshold behavior in 7075 aluminum alloy [J]. International Journal of Fatigue, 1999, 21(S1): s255−s262.

焊后热处理对 AA2219 铝合金变极性 TIG 焊接头性能的影响

丁吉坤[1,2]，王东坡[1,2]，王 颖[1,2]，杜 辉[1,2]

1. 天津大学 材料科学与工程学院，天津 300072；
2. 天津市现代连接技术重点实验室，天津 300072

摘 要：采用变极性 TIG 焊接方法制备 AA2219 铝合金焊接接头，研究焊后热处理对接头的拉伸、微观组织和疲劳性能的影响。变极性 TIG 焊具有在保证阴极清理作用的前提下最大限度地降低对钨极的烧损的优点。焊接试样分为原始焊态试样和热处理态试样两种。热处理方案采用固溶处理(535 °C，30 min)、水冷淬火和人工时效(175 °C，12 h)。结果表明，焊后热处理能够显著地提高原始焊态试样的力学性能(屈服强度提高 42.6%，抗拉强度提高 43.1%)，改善微观组织以及提高抗疲劳性能(疲劳强度提高 18.4%)。

关键词：AA2219 铝合金；变极性 TIG 焊；焊后热处理；力学性能；微观组织；疲劳性能

(Edited by Hua YANG)